

Regional-scale paleoclimate influences on a proposed Deep Geologic Repository in Canada for low and intermediate level waste

S.D. Normani, J.F. Sykes & Y.Yin

University of Waterloo, Waterloo, Ontario, Canada

ABSTRACT: A Deep Geologic Repository (DGR) for Low and Intermediate Level radioactive waste has been proposed by Ontario Power Generation for the Bruce Nuclear site in Ontario, Canada. The DGR is to be constructed at a depth of about 680 m below ground surface within the argillaceous Ordovician limestone of the Cobourg Formation. The objective of this paper is to apply paleoclimate boundary conditions to a regional-scale groundwater flow model for the DGR site and to describe the influence of glacial loading and unloading on flow system evolution using the FRAC3DVS-OPG flow and transport model. The regional-scale domain encompasses an area of 18,775 km² extending from Lake Huron to Georgian Bay in southwestern Ontario, Canada.

From a hydrogeologic perspective, the domain can be subdivided into a shallow zone, an intermediate zone, and a deep zone comprised of the low-permeability units of Ordovician and the more permeable Cambrian where present. The deep groundwater zone is characterized by units containing stagnant water having high concentrations of total dissolved solids (TDS) that can exceed 300 g/L. The high TDS values at depth require density-dependent coupled flow and transport calculations within FRAC3DVS-OPG. The computational sequence involves the calculation of steady-state density independent flow that is used as the initial condition for the determination of pseudo-equilibrium for a density-dependent flow system that has an initial TDS distribution. The 1,000,000 year pseudo-equilibrium heads and brine concentrations are used as the initial condition for the paleoclimate simulations.

Over the past 900,000 years, the Canadian Shield has experienced approximately nine episodes of complete glaciation. During the glaciation cycles, the entire Canadian land mass has been covered by a series of continental ice-sheets whose maximum thickness reached 4 km and whose southern extents reached, in some cases, beyond the present-day Canada-U.S. border. The glaciation phase of a single glaciation-deglaciation episode is typically 90,000 years in duration, while the deglaciation portion proceeds relatively rapidly and has an average duration of approximately 10,000 years. Output from the University of Toronto Glacial Systems Model, a continental scale North American glacial reconstruction of the most recent 120,000 year glaciation event developed by W. R. Peltier, is used to supply the paleoclimate boundary conditions used in this paper. Permeability reductions due to the presence of permafrost are also considered in the paleoclimate simulations. This paper will demonstrate that the choice of rock properties can significantly affect residual pore water pressures within the rock matrix, as well as the migration of glacial meltwater.

1 INTRODUCTION

A Deep Geologic Repository (DGR) for Low and Intermediate Level (L&IL) radioactive waste has been proposed by Ontario Power Generation (OPG) for the Bruce site on the shore of Lake Huron near Tiverton, Ontario (Figure 1). The DGR is to be excavated at a depth of approximately 680 m within the argillaceous limestone of the Ordovician Cobourg Formation. In order to reasonably assure safety of the radioactive waste at the site and to better understand the geochemistry and hydrogeology of the formations surrounding the proposed DGR, a regional-scale and site-scale

numerical modelling study has been completed in Sykes et al. (2008); the paleoclimate portions of the regional-scale modelling are reported in this paper. This numerical modelling study provides a framework to investigate the groundwater flow system as it relates to and potentially affects the safety and long-term performance of the DGR.

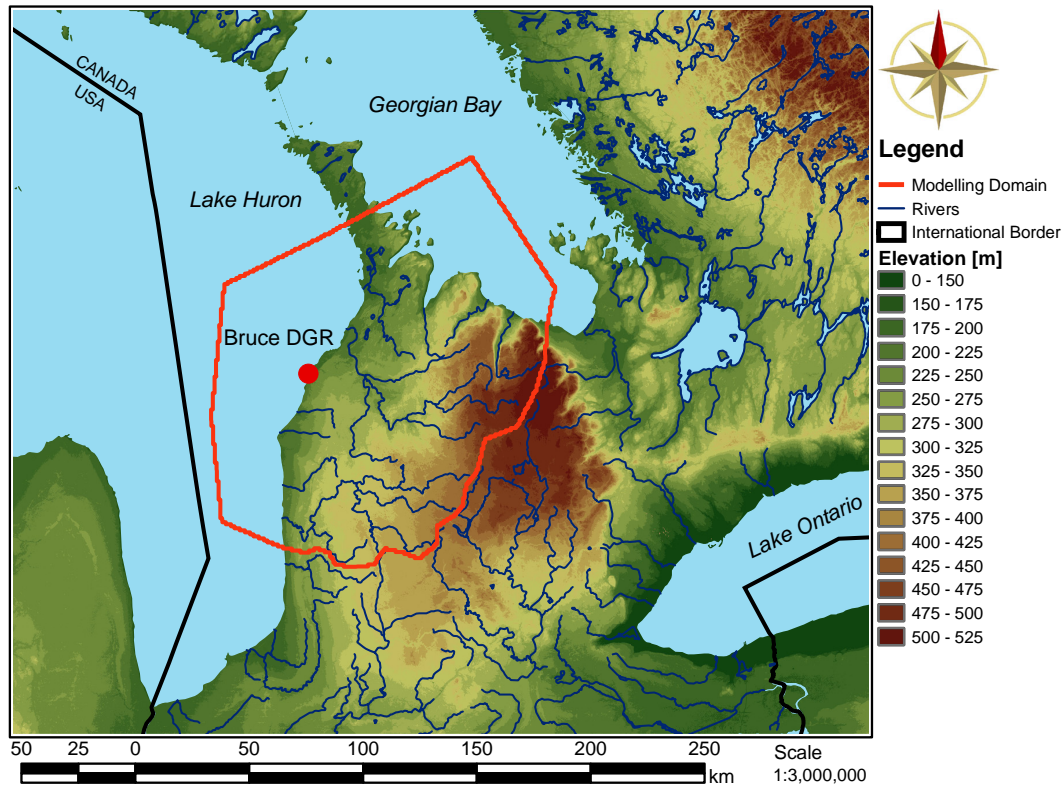


Figure 1. Regional-scale elevations, river courses, and location of DGR site in southwestern Ontario.

In order to capture and recreate the regional-scale groundwater system, in both near-surface and deep environments, a groundwater flow model is developed, using FRAC3DVS-OPG (developed from FRAC3DVS (Therrien et al. 2004)), for a fully three-dimensional representation of the bedrock stratigraphy within a portion of south-western Ontario centered on the Bruce DGR site. From a hydrogeologic perspective, the domain at the Bruce site can be subdivided into three horizons: a shallow zone characterized by the dolomite and limestone units of the Devonian that have higher permeability and groundwater composition with a relatively low total dissolved solids content; an intermediate zone comprised of the low permeability shale, salt and evaporite units of the Upper Silurian, the more permeable Niagaran Group (including the Guelph, Goat Island and Gasport) and the Lower Silurian carbonates and shales; and a deep groundwater zone extending to the Precambrian and characterized by the Ordovician shales and carbonate formations and the Cambrian sandstones and dolomites. Pore water in the deeper zone is thought to be stagnant and has high total dissolved solids (TDS) concentrations that can exceed 300 g/L with a corresponding specific gravity of 1.2 for the fluids. In this paper, the term stagnant is used to define groundwater in which solute transport is dominated by molecular diffusion.

2 GOVERNING EQUATIONS

The saturated, density-dependent form of Darcy's Law is given by:

$$q_i = -\frac{k_{ij}}{\mu} \left(\frac{\partial p}{\partial x_j} + \rho g \eta_j \right) \quad (1)$$

where q_i [$L T^{-1}$] is the flux in the i th direction, k_{ij} [L^2] is the permeability tensor, μ is the viscosity [$M L^{-1} T^{-1}$], p [L] is the pressure, ρ [$M L^{-3}$] is the density of groundwater and $\eta = 1$ [L] for the vertical (z) direction, while $\eta = 0$ for the horizontal directions (x and y). When Equation (1) is rewritten in terms of equivalent freshwater heads (which is defined as follows: $h = p/\rho_0g + z$), it becomes:

$$q_i = -\frac{k_{ij}}{\mu g} \left(\frac{\partial h}{\partial x_j} + \rho_r \eta_j \right) \quad (2)$$

where ρ_r [dimensionless] is the relative density, given by $\rho/\rho_0 - 1$ where ρ_0 is the reference freshwater density. For elastic fluids, the density of a fluid becomes a function of the fluid pressure and solute concentration:

$$\rho = \rho_0 [1 + c_w (p - p_0) + \gamma C] \quad (3)$$

where ρ_0 [$M L^{-3}$] is the freshwater density at a reference pressure p_0 , c_w is the compressibility of water, γ is a constant derived from the maximum density of the fluid, ρ_{max} and is defined as $\gamma = (\rho_{max}/\rho_0 - 1)$ and C is the relative concentration.

Under isothermal conditions, the viscosity μ is a function of the concentration of the fluid. For the viscosity, it is assumed that there is a linear relation between the relative concentration so long as the maximum viscosity change is insignificant in isothermal conditions.

$$\mu = \mu_0 (1 + \gamma_\mu C) \quad (4)$$

where μ_0 is the viscosity of freshwater and $\gamma_\mu = (\mu_{max}/\mu_0 - 1)$. When the equations for the elasticity of the fluid and the viscosity are included in the Darcy's equation, it becomes:

$$q_i = -\frac{k_{ij}}{\mu_0 g} \cdot \frac{1}{1 + \gamma_\mu C} \left(\frac{\partial h}{\partial x_j} + [c_w (p - p_0) + \gamma C] \eta_j \right) \quad (5)$$

The groundwater flow equation can then be derived using Equation (5) and the continuity of energy principle.

$$\frac{\partial}{\partial x_i} \left[K_{ij}^0 \cdot \frac{1}{1 + \gamma_\mu C} \left(\frac{\partial h}{\partial x_j} + [c_w (p - p_0) + \gamma C] \eta_j \right) \right] = S_s \frac{\partial h}{\partial t} \quad (6)$$

where $K_{ij}^0 = k_{ij}/\mu_0 g$ and S_s is the specific storage term.

The solute continuity equation is written in terms of relative concentration as:

$$\frac{\partial}{\partial x_i} \left(\phi D_{ij} \frac{\partial C}{\partial x_j} \right) - \frac{\partial}{\partial x_i} (q_i C) = \phi \frac{\partial C}{\partial t} \quad (7)$$

where the Darcy flux q_i is computed by solving Equation (6), ϕ is the porosity and D_{ij} is the hydrodynamic dispersion tensor (Bear 1988):

$$\phi D_{ij} = (\alpha_l - \alpha_t) \frac{q_i q_j}{|q|} + \alpha_t |q| \delta_{ij} + \phi \tau D_w \delta_{ij} \quad (8)$$

where α_l and α_t are the longitudinal and transverse dispersivities respectively, $|q|$ is the magnitude of the Darcy flux, τ is the tortuosity, D_w is the free solution diffusion coefficient or simply the diffusion coefficient and δ_{ij} is the Kronecker delta. The pore water diffusion coefficient is obtained by τD_w . In literature, the pore water diffusion coefficient is also referred to as the diffusion coefficient of the porous medium (Bear 1988).

It should be noted that the equations for density-dependent flow and transport are nonlinear; to solve the flow Equation (6), the relative densities, which are dependent upon the transport Equation (7), which itself requires Darcy fluxes from Equation (6), are required. For more detail on the implementation of density-dependent flow in FRAC3DVS, refer to Therrien et al. (2004).

3 MODEL DEVELOPMENT

The regional scale domain, shown in Figure 1, occupies an aerial extent of approximately 18,775 km². It has vertical elevations that range from –1000 m at the lowest point in the Precambrian to 539 m at the highest point on the Niagara Escarpment. The domain was discretized into slices with 27,728 nodes each, which were then used to create quadrilateral elements. Based on an areal discretization with 200 rows and 200 columns, these quadrilateral elements have sides of 762.8 m in the East-West direction by 900.9 m in the North-South direction. Each of the 31 units from the geological reconstruction was assigned a model layer so that the numerical model would closely resemble that of the geological framework model. This resulted in 31 layers in the numerical model. The elevation of the nodes for each slice were determined from the GLL00 geological framework model described in Frizzell et al. (2008). Each geologic interface in the geological framework model, representing the top of a geologic formation or unit, is comprised of a triangulated surface mesh. A computer script was written to interpolate the elevation of the slice nodes from the appropriate layer of the geological framework model.

3.1 Flow Boundary and Initial Conditions

The boundary conditions of the model were Neumann no-flow boundary conditions for the sides and bottom, and type-one or Dirichlet for the surface of the model. The elevation of the nodes at the top of the model domain are defined by either the DEM or the lake bathymetry. For surface nodes with an elevation greater than 176 m, the assigned prescribed head was set as the elevation minus 3 m but not less than the 176 m Lake Huron water elevation. Areas within the domain that are occupied by either Lake Huron or Georgian Bay have a prescribed equivalent freshwater head for the top slice of the model matching the lake elevation, 176 m. The imposed surface boundary condition permits recharge and discharge to occur as determined by the surface topography and the hydraulic conductivity of the top model layer. The assigned head represents a water table occurring at an assumed depth of 3 m below ground surface. Because of the resolution of the DEM, stream channels are conceptualized to have a depth to water that is 3 m less than defined by the DEM.

In the absence of a source that can generate salt and hence total dissolved solids, the simulation of density-dependent flow using coupled flow and transport equations requires a transient analysis. The initial equivalent freshwater head distribution for the analysis was determined as the steady-state solution of density-independent flow subject to the same flow boundary conditions as that of the transient analysis.

3.2 Hydraulic and Transport Parameters

The base-case data set for the conceptual model consists of 31 model layers, with each layer corresponding to a unit in the stratigraphic section. Table 1 shows the layers and their associated hydraulic conductivities, porosities and specific storage coefficients. While numbers in the table are reported to two digit accuracy, it is recognized that the second digit may be beyond the accuracy of field measurement techniques. The porosity values were developed from data compiled by Golder Associates Limited (2003) and revised as appropriate by data from the Bruce site field program. The horizontal hydraulic conductivity for the shallow drift layer was assigned a value of 1×10^{-7} m/s.

Following Freeze & Cherry (1979), the specific storage coefficient can be developed as:

$$S_s = \rho g (C_r + \phi C_w) \quad (9)$$

where ρ is the fluid density, g is the gravitational constant, C_w is the compressibility of the fluid, ϕ is the porosity and C_r is the rock compressibility. The specific storage coefficients listed in Table 1 were derived using the fluid densities corresponding to a unit's TDS concentration, the unit's porosity and the appropriate compressibility from Table 2.

To simulate the impact that a weathered zone will have on shallow flow, the upper 20 metres of the spatial domain was assumed to be characterized by more permeable rock; the horizontal hydraulic conductivity for the zone was assumed to be 1×10^{-7} m/s. The anisotropy ratios of Table 1 were assumed to be applicable.

Table 3 gives the parameters assumed for both the migration of total dissolved solids and for the estimation of mean life expectancy. Using a grid Peclet number constraint, the longitudinal dispersivity coefficient was selected as approximately one half of the maximum length of the side of a regional-scale grid block. The diffusion coefficient is listed in the table; temperature effects were not considered.

3.3 Total Dissolved Solids

Salinity plays an important role with regard to fluid flow at the proposed DGR. An increase in the concentration of total dissolved solids (TDS) will result in an increase in the fluid density. The increase in density of the deeper fluids will then act as an inhibitor of active flow at depth.

The spatial distribution of TDS concentration in the units of the Ontario portion of the Michigan Basin have been compiled in studies by Golder Associates Limited (2003) and Hobbs et al. (2008). The values listed in Table 4 represent the average of the minimum and maximum values reported for given units. For the analyses presented in this paper using the GLL00 geological framework model, the initial TDS distribution (refer to Table 4) was assigned based on site specific field data; the concentrations correspond to the higher values reported for a given unit from both the Golder Associates Limited (2003) and Hobbs et al. (2008) studies. These concentrations will be redistributed in a density-dependent flow analysis and in parts of the domain they will be diluted by infiltrating fresh water. The use of the maximum TDS concentrations for a unit is therefore appropriate as an initial condition. Finally, the geological framework model integrates the various units of the Niagaran Group into a single layer; only a single TDS value is given for that layer in Table 4.

After 1 million years, the model, having been allowed to reach pseudo-equilibrium, produces salinity profiles that are compatible with the geological framework, boundary conditions and hence the flow domain. In the north-eastern part of the model domain, the brine will be unable to accumulate because of a combination of the absence of the source term and the effect of meteoric recharge near Georgian Bay where the Ordovician formations outcrop. This is contrasted by the western portion of the domain which, because of the absence of a velocity to transport the brine from the system, will maintain a high salinity concentration. The location of the proposed DGR repository is located within this area. At such a location, stagnation of the groundwater is expected due to both the low permeability of the Ordovician units and the effect that density will have on reducing the flow velocity.

3.4 Implementation of Paleoclimate and Surface Boundary Conditions

The climate and surface boundary conditions are provided by Peltier (2008). Two parameters are used in this study: permafrost depth (d_{PF}), and the normal stress (σ_{ice}) at ground surface due to the presence of ice. Both of these parameters are used, with some assumptions, in FRAC3DVS-OPG. Firstly, the ice load is applied as equivalent freshwater head using a Dirichlet boundary condition across all surface nodes. Assuming purely vertical strain and areally homogeneous loading, the ice stress also is used to modify the pore pressure of the rock as would occur with its compression on loading and dilation on load removal (Neuzil 2003). Secondly, the permafrost depth modifies the porous media hydraulic conductivity depending on the depth of permafrost. Both permafrost depth and normal stress vary in time with 500 year time steps. FRAC3DVS-OPG can vary time steps to suit groundwater flow and solute transport maximum change criteria.

The equations that describe the impact of glaciation and deglaciation on groundwater pressures and flow can be simplified by assuming that ice loads are areally homogeneous in which case, the lateral strains are zero. The assumption is valid for cases where the speed of advance and retreat of the glacier is fast relative to the horizontal flow velocity in the groundwater system. For this case of purely vertical strain and following the development of Neuzil (2003), the density-dependent flow equation becomes:

$$\frac{\partial}{\partial x_i} \left[K_{ij}^0 \cdot \frac{1}{1 + \gamma_\mu C} \left(\frac{\partial h}{\partial x_j} + [c_w(p - p_0) + \gamma C] \eta_j \right) \right] = S_s \frac{\partial h}{\partial t} - S_s \zeta \frac{\partial \sigma_{zz}}{\partial t} \quad (10)$$

where σ_{zz} is the vertical stress. The one-dimensional loading efficiency, ζ , is a function of Poisson's ratio for the rock, the drained bulk modulus of the porous medium, the modulus of the solids

Table 1. Material hydraulic properties for regional-scale analysis.

Period	Geology	K_H [m/s]	K_V [m/s]	K_V/K_H	Porosity	Specific Stor.
Quaternary	Drift	1.0×10^{-7}	2.0×10^{-8}	0.2	0.10	9.9×10^{-5}
Devonian	Traverse Group	1.0×10^{-7}	1.0×10^{-8}	0.1	0.10	9.9×10^{-5}
	Dundee	1.0×10^{-7}	1.0×10^{-8}	0.1	0.10	9.9×10^{-5}
	Detroit River Group	1.0×10^{-7}	1.0×10^{-8}	0.1	0.10	1.4×10^{-6}
	Bois Blanc	1.0×10^{-7}	1.0×10^{-8}	0.1	0.10	1.4×10^{-6}
Silurian	Bass Islands	1.0×10^{-7}	1.0×10^{-8}	0.1	0.10	1.4×10^{-6}
	G-Unit	1.0×10^{-7}	1.0×10^{-8}	0.1	0.08	1.3×10^{-6}
	F-Unit	4.0×10^{-12}	4.0×10^{-13}	0.1	0.03	1.2×10^{-4}
	F-Salt	1.0×10^{-13}	1.0×10^{-13}	1.0	0.08	1.6×10^{-6}
	E-Unit	4.0×10^{-12}	4.0×10^{-13}	0.1	0.08	1.6×10^{-6}
	D-Unit	1.0×10^{-10}	1.0×10^{-11}	0.1	0.03	1.3×10^{-6}
	B&C Units	4.0×10^{-12}	4.0×10^{-13}	0.1	0.08	1.2×10^{-4}
	B Anhydrite-Salt	1.0×10^{-13}	1.0×10^{-13}	1.0	0.08	1.6×10^{-6}
	A2-Carbonate	1.0×10^{-10}	1.0×10^{-11}	0.1	0.08	1.6×10^{-6}
	A2 Anhydrite-Salt	1.0×10^{-13}	1.0×10^{-13}	1.0	0.08	1.6×10^{-6}
	A1-Carbonate	2.0×10^{-12}	2.0×10^{-13}	0.1	0.08	1.6×10^{-6}
	A1-Evaporite	1.0×10^{-13}	1.0×10^{-13}	1.0	0.08	1.6×10^{-6}
	Niagaran	1.0×10^{-7}	1.0×10^{-8}	0.1	0.08	1.6×10^{-6}
	Fossil Hill	2.0×10^{-11}	2.0×10^{-12}	0.1	0.08	1.6×10^{-6}
	Cabot Head	2.0×10^{-12}	2.0×10^{-13}	0.1	0.03	1.2×10^{-4}
Manitoulin	1.5×10^{-12}	1.5×10^{-13}	0.1	0.01	1.2×10^{-6}	
Ordovician	Queenston	1.3×10^{-11}	1.3×10^{-12}	0.1	0.11	1.2×10^{-4}
	Georgian Bay/Blue Mtn.	9.1×10^{-12}	9.1×10^{-13}	0.1	0.11	1.2×10^{-4}
	Cobourg	9.6×10^{-12}	9.6×10^{-13}	0.1	0.02	1.3×10^{-6}
	Sherman Fall	9.0×10^{-12}	9.0×10^{-13}	0.1	0.02	1.3×10^{-6}
	Kirkfield	1.4×10^{-11}	1.4×10^{-12}	0.1	0.02	1.3×10^{-6}
	Coboconk	5.2×10^{-11}	5.2×10^{-12}	0.1	0.02	1.3×10^{-6}
	Gull River	3.6×10^{-11}	3.6×10^{-12}	0.1	0.02	1.3×10^{-6}
	Shadow Lake	8.0×10^{-12}	8.0×10^{-13}	0.1	0.01	1.2×10^{-6}
Cambrian	Cambrian	3.0×10^{-6}	3.0×10^{-7}	0.1	0.01	1.2×10^{-6}
Precambrian	Precambrian	8.0×10^{-12}	8.0×10^{-13}	0.1	0.01	1.2×10^{-6}

Table 2. Fluid and rock compressibilities

Material	Compressibility [Pa^{-1}]
Fluid	4.4×10^{-10}
Sandstone	1×10^{-10}
Limestone	1×10^{-10}
Dolomite	1×10^{-10}
Shale	1×10^{-8}
Precambrian	1×10^{-10}

Table 3. Transport parameters

Parameter	Value
Tortuosity	1.0
Diffusion Coefficient	$1.2 \times 10^{-10} \text{ m}^2/\text{s}$
Longitudinal Dispersivity	500m
Transverse Dispersivity/Longitudinal Dispersivity	0.1
Vertical Transverse Dispersivity/Longitudinal Dispersivity	0.01

Table 4. Initial TDS and relative concentrations with respect to 300 g/L for base case parameters and GLL00 geology

Period	Geology	GLL00 Geology	
		TDS [g/L]	Relative Conc.
Quaternary	Drift	0.045	0.0
Devonian	Traverse Group	0.045	0.0
	Dundee	3	0.01
	Detroit River Group *	3	0.01
	Bois Blanc	3	0.01
Silurian	Bass Islands	3	0.01
	G-Unit	3	0.01
	F-Unit	300	1.0
	F-Salt	300	1.0
	E-Unit	300	1.0
	D-Unit	300	1.0
	B&C Units	300	1.0
	B Anhydrite-Salt	300	1.0
	A2-Carbonate	300	1.0
	A2 Anhydrite-Salt	300	1.0
	A1-Carbonate	300	1.0
	A1-Evaporite	300	1.0
	Niagaran **	300	1.0
	Fossil Hill	300	1.0
Cabot Head	300	1.0	
Manitoulin	300	1.0	
Ordovician	Queenston	300	1.0
	Georgian Bay/Blue Mtn.	300	1.0
	Cobourg	300	1.0
	Sherman Fall	300	1.0
	Kirkfield	300	1.0
	Coboconk	300	1.0
	Gull River	300	1.0
	Shadow Lake	300	1.0
Cambrian	Cambrian	300	1.0
Precambrian	Precambrian	300	1.0

* Includes the Lucas/Amherstburg Formations

** The Niagaran Group is comprised of the Guelph, Goat Island, Gasport and Lions Head Formations

and the porosity. Values for the one-dimensional loading efficiency vary between zero and one. When ζ equals zero, Equation (10) is equal to Equation (6). The last term in Equation (10) is independent of the equivalent freshwater head h and modifies the pressure throughout the one-dimensional column beneath the surface ice by adding water on loading and extracting water on unloading with the volume of water being defined by the porosity and compressibility terms in the specific storage.

The hydraulic conductivity of frozen porous media is assigned the value of 1.6×10^{-3} m/year (5×10^{-11} m/s) and is assumed to be isotropic (McCauley et al. 2002). For each time step, if the depth of permafrost extends below the top of an element, calculated at the centroid of the top face, that element will be assigned the permafrost permeability. The normal stress due to the weight of ice on the domain is used to calculate an equivalent freshwater head which is applied at all surface nodes as a Dirichlet boundary condition, h_{ice} according to:

$$h_{ice} = \frac{\sigma_{ice}}{\rho g} + z \quad (11)$$

where ρ is freshwater density, g is the gravitational constant, and z is elevation of the water table, itself located 3 m below ground surface and also specified using a Dirichlet boundary condition for most modelling scenarios. If $\sigma_{ice} = 0$, then the specified head is defined as in the non paleoclimate simulations. A meltwater production rate is not used for the ice-sheet.

4 LONG-TERM CLIMATE CHANGE

The effects of long-term climate change (e.g. permafrost) on the groundwater flow system are investigated by modifying the permeability of rock within the permafrost zone, by changing the surface boundary conditions to reflect a glacial scenario, and depending on the loading efficiency (refer to Equation (10)), by the inclusion of a pressure modifying term in the flow equation using the methodology described in Section 3.4.

Using the deterministic University of Toronto Glacial Systems Model (GSM) of continental ice-sheet evolution, Peltier (2008) focuses on eight of the models of the ensemble that span the apparent range of model characteristics that provide acceptable fits to the totality of the observational constraints. Of the models, nn9930 was chosen for the paleoclimate analysis in this paper. A plot of permafrost depth and ice load, expressed as equivalent metres of water, is shown in Figure 2 for the nn9930 glaciation scenario and the location of the proposed DGR. Two glaciation events were predicted to occur over the regional-scale domain with the first event spanning a period from approximately -62.5 kyr to -56 kyr and the most recent event occurring in the period from approximately -24 kyr to -13 kyr. Permafrost occurs approximately 12 kyr to 14 kyr prior to the onset of glaciation and is fully absent approximately 1 kyr after onset. While Peltier (2008) provides estimates from the nn9930 glaciation scenario of the basal meltwater production and the lake depth at the location of the proposed DGR, these data are not used in the simulations of this paper.

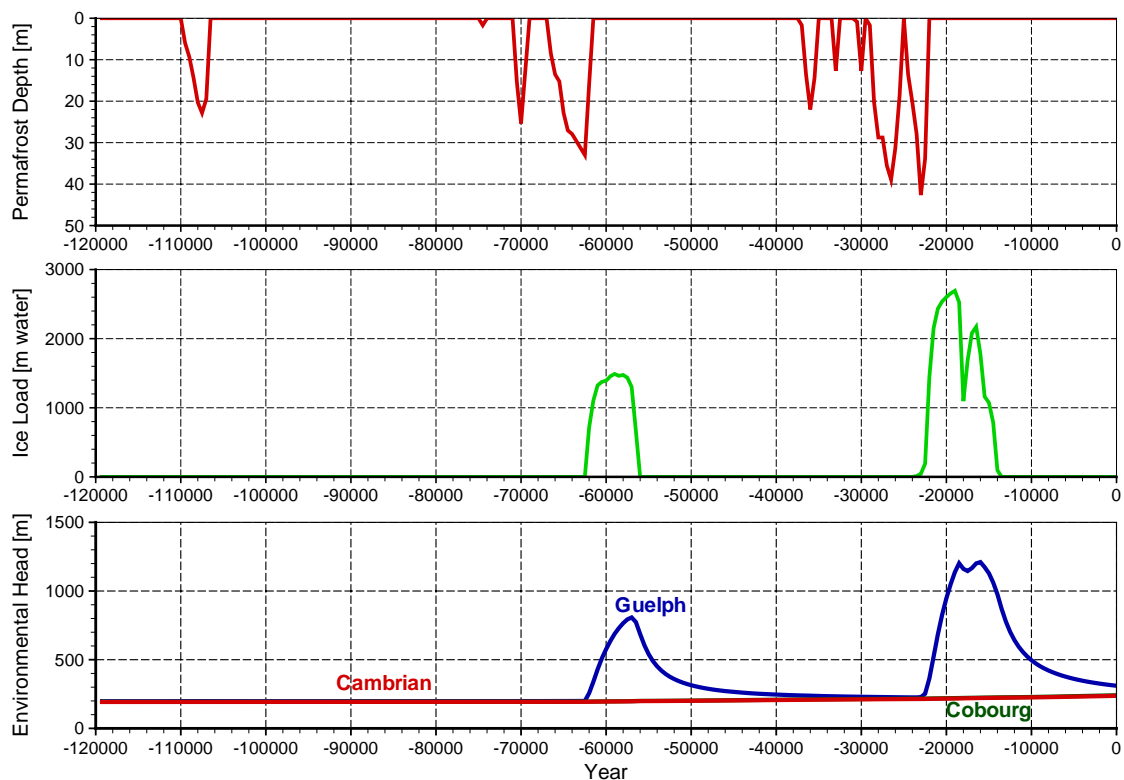


Figure 2. Time series plots of (a) permafrost depth, (b) ice load in equivalent metres of water for climate simulation nn9930, and (c) simulated environmental heads in the Guelph Formation of the Niagaran Group, Cobourg and Cambrian for a loading efficiency of zero.

Zero flux Neumann boundary conditions were used for the lateral and bottom surfaces of the model domain. A Dirichlet boundary condition was applied to the upper surface as described in Section 3.4. The ice loading was assumed to be applied as an equivalent freshwater head equal to the normal stress imposed by the ice sheet upon the domain. It was also incorporated as a pressure modifying term throughout the domain that, with the assumption of vertical strain and homogeneous loading, approximates the impact of the applied load on the rock. As described in Equation (10), this term includes a loading efficiency ζ ; a loading efficiency of zero ($\zeta = 0$) and a loading efficiency of one ($\zeta = 1$) were applied. Although FRAC3DVS-OPG does not rigorously account for hydro-mechanical effects, this analysis does demonstrate the behaviour of deep groundwater flow systems subjected to permafrost conditions and glacial loading events and provides a basis to qualitatively understand the magnitude and time rate-of-change of flow in response to ice-sheet advance and retreat.

Basal meltwater and pro-glacial lakes could result in the penetration of oxygenated recharge waters to depth during and following a glaciation event. To analyze this situation, a unit load of concentration was applied at the surface nodes of the regional-scale numerical model. Recharge occurring during the 120,000 year simulation is thereby tagged with a tracer of unit concentration.

The paleoclimate scenario nn9930 for the location of the proposed DGR is shown in Figure 2. The environmental heads at present, following the 120,000 year paleoclimate simulation, are shown in Figure 3. A block-cut diagram of the velocity magnitude at the present is shown in Figure 4. The tracer concentration distribution in the regional-scale domain at the present is shown in Figure 5.

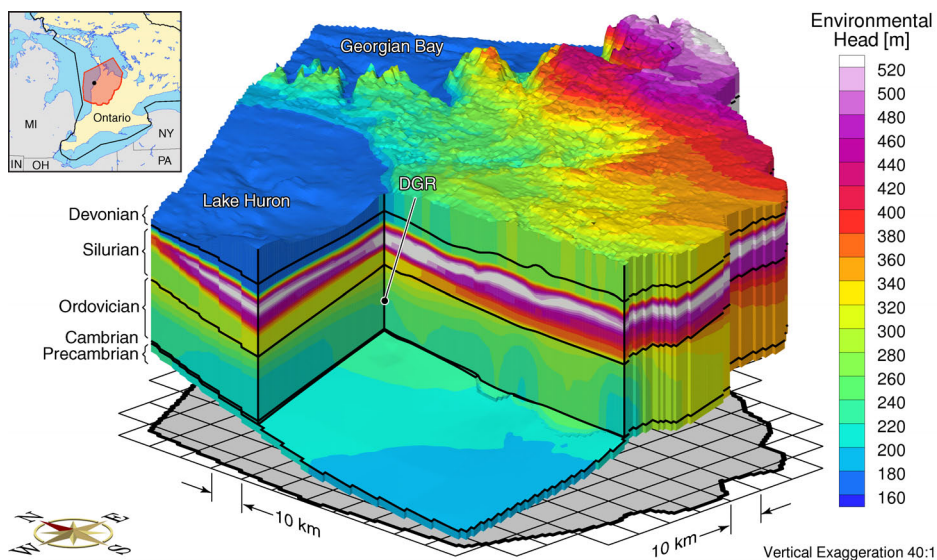


Figure 3. Environmental heads at the present for the base case parameters and a loading efficiency of zero.

Since the loading efficiency is zero, there is no impact on the pore pressure at depth from the compression of the rock under ice loading. The ice load is assumed to impact only the surface pore pressure. This increased surface pressure propagates into the domain at a rate depending on the temporal loading, permafrost depth and properties, fluid compressibility, rock compressibility and the hydraulic conductivity distribution. The resulting energy gradient into the domain is maximum for a loading efficiency of zero ($\zeta = 0$). A higher loading efficiency will result in increased pore pressures throughout the rock column as the rock is compressed, the impact is to reduce the vertically downward energy gradient. On de-glaciation, the pore pressure at the domain surface is reduced and the pore pressure throughout the rock column is correspondingly relieved by the ice stress term in Equation (10). A consequence of a maximum pore pressure energy gradient is maximum penetration of basal meltwater into the domain. The tracer concentration distribution at the end of the 120 kyr simulation is shown in Figure 5. At the location of the DGR, glacial meltwater has not penetrated through the low permeability units of the Salina.

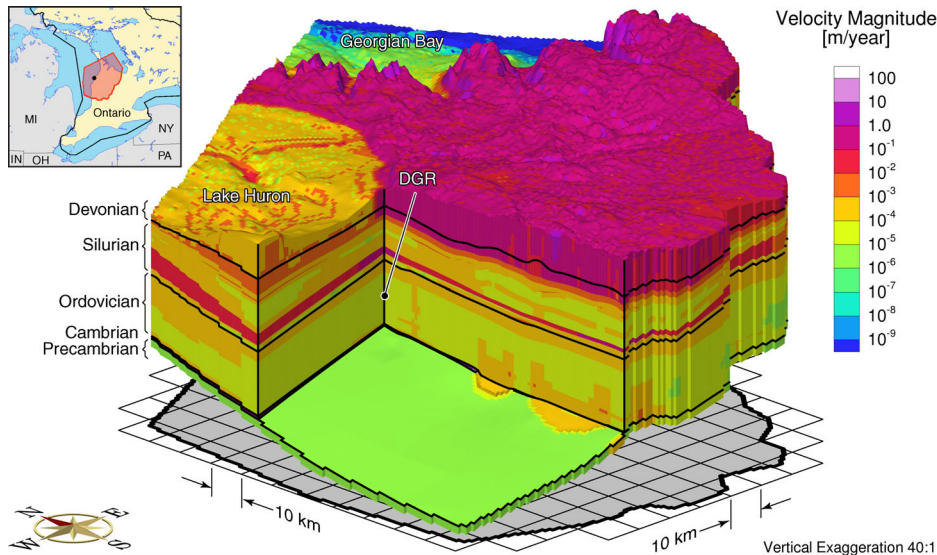


Figure 4. Block-cut diagram showing pore water velocity magnitude at the present for the base case parameters and a loading efficiency of zero.

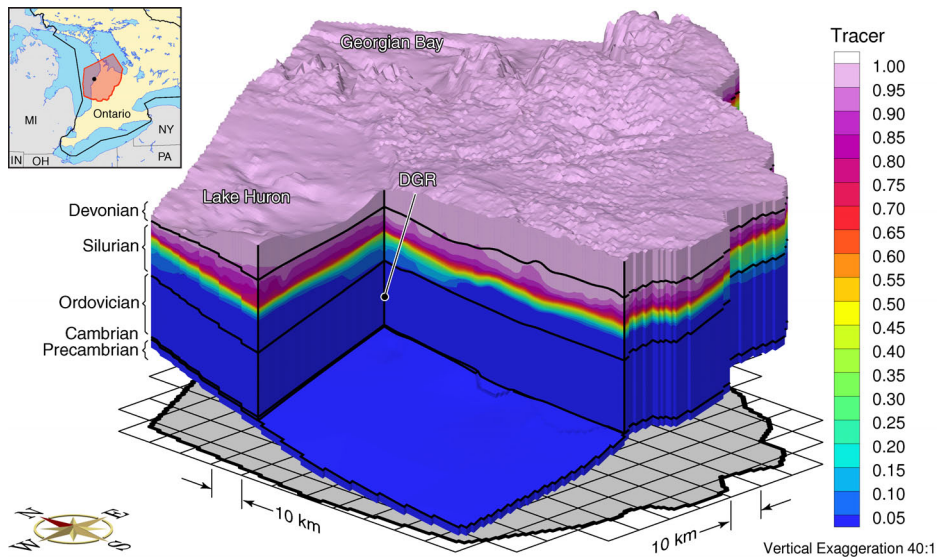


Figure 5. Block-cut diagram showing the depth of penetration of a tracer at the present for the base case parameters and a loading efficiency of zero.

A review of the temporal and spatial distributions of the environmental head reveals that the higher permeability Niagaran is an important pathway for the propagation of the glaciation surface pressures to depth. With a loading efficiency of zero, higher pressures in the unit occur where it outcrops; lower pressures are at depth. The high pressures are transmitted down dip through the unit to the areas overlain by the confining Salina units. The result is that the low permeability Salina receives a high pressure pulse from the Devonian units above and from the underlying Niagaran. These higher pressures propagate vertically into the Salina resulting in it becoming over-pressured with respect to the surface elevation. The residual signature of these higher pressures is evident in Figure 3 as the white to red environmental heads at the midpoint of the Silurian. The temporal change in the environmental heads in the Niagaran Formation, Cobourg Formation and Cambrian Formation at the location of the proposed DGR are shown in Figure 2. It is evident in both this plot and Figure 3 that for a loading efficiency of zero, the low permeability of the Lower Silurian and Ordovician units, the specific storage coefficients for the units and the duration of the glacial loading, that the higher pressures in the Niagaran and Devonian cannot propagate to depth. As shown in Figure 2 there is a large vertically downward gradient between the Niagaran

and the lower units. The length of glaciation and de-glaciation for scenario nn9930 is not long enough for the tracer to migrate down dip in the Niagaran to the location of the proposed DGR.

The temporal change in the environmental heads in the Niagaran, Cobourg and Cambrian at the location of the proposed DGR is shown in Figure 6 (note that the Niagaran is referred to as the Guelph in the figure) for a loading efficiency of one ($\zeta = 1$) in Equation (10). As shown in the figure, the impact of the stress term with a loading efficiency of one is an increase in pore pressure with rock compression during glaciation and a decrease in the rock pore pressure as the rock dilates during de-glaciation. The vertical energy gradient is significantly reduced compared to that of the case with a loading efficiency of zero (refer to Figure 2). At the peak loading of the second glaciation event at -19.5 kyr, the environmental heads in the Cambrian and Niagaran (Guelph in the figure) were estimated to be 2905 m and 2837 m respectively. The small upward gradient with $\zeta = 1$ compares to a large downward gradient being predicted at the same time for the case with $\zeta = 0$. Also of note in the figure is the fact that Equation (10) with ($\zeta = 1$) results in no latency in the dissipation of the elevated pressures after complete de-glaciation. The results of Figure 2 and Figure 6 provide the bounding cases for the formulation of Equation (10).

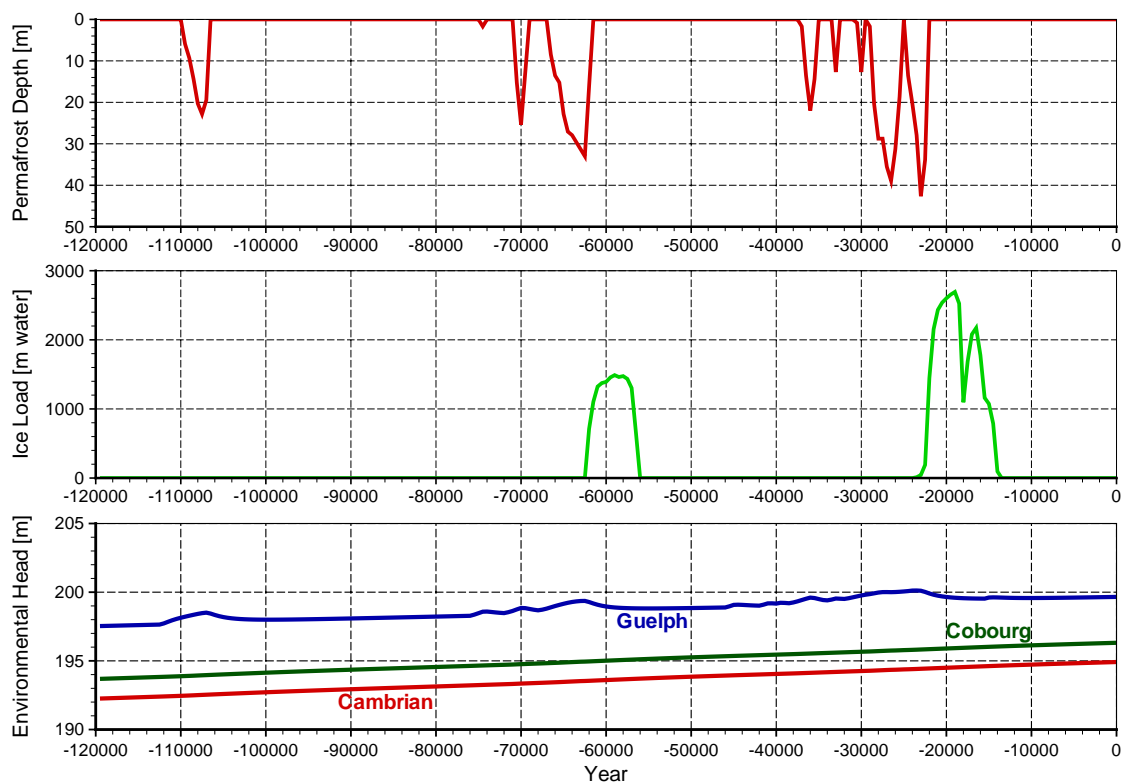


Figure 6. Time series plots of (a) permafrost depth, (b) ice load in equivalent metres of water for climate simulation nn9930, and (c) simulated environmental heads in the Guelph Formation of the Niagaran Group, Cobourg and Cambrian for a loading efficiency of one.

In Figure 7, the depth of tracer migration is noticeably less than in Figure 5. This is a further indication of the significantly reduced vertical gradients that result from including hydromechanical coupling in paleoclimate simulations. Based on these simulations, paleoclimate simulations that do not account for hydromechanical effects on pore water pressures can significantly overestimate the vertical gradients, thereby enhancing migration of surface waters deep into the subsurface environment.

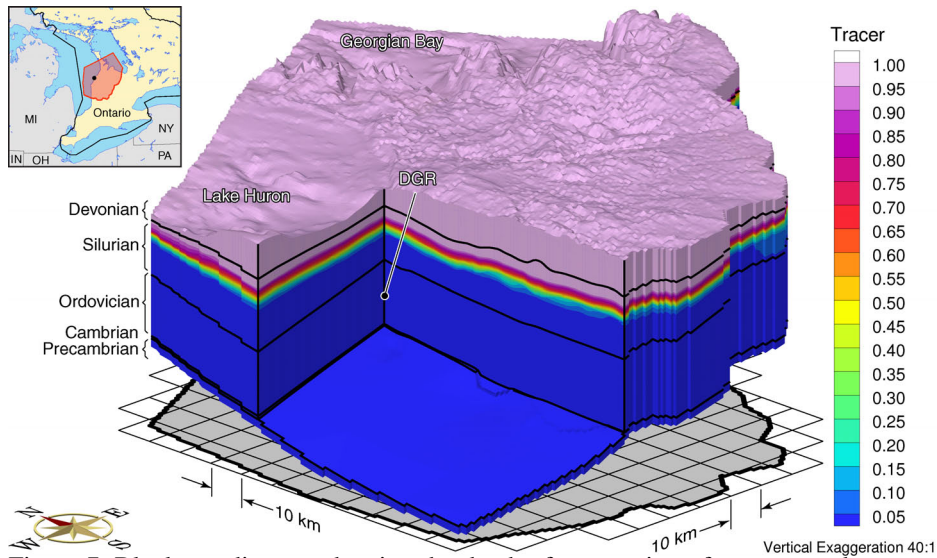


Figure 7. Block-cut diagram showing the depth of penetration of a tracer at the present for the base case parameters and a loading efficiency of one.

5 CONCLUSIONS

This paper has shown the importance of including hydromechanical coupling for paleoclimate simulations. Simulation results show that hydromechanical coupling reduces vertical pore water gradients during glacial loading and unloading, thereby reducing fluxes into or out of the subsurface. Paleoclimate simulations that do not account for hydromechanical effects on pore water pressures can significantly overestimate the vertical gradients, thereby enhancing migration of surface waters deep into the subsurface environment. Rock compressibilities also affect calculated storage coefficients which allow elevated pore pressures generated during glacial loading to remain, and slowly dissipate once the glacial episode has ended.

REFERENCES

- Bear, J. 1988. *Dynamics of Fluids in Porous Media*. Dover edition. Dover Publications Inc.
- Freeze, R.A. & Cherry, J.A. 1979. *Groundwater*. Englewood Cliffs, N.J.: Prentice-Hall, Inc.
- Frizzell, R., Cotesta, L. & Usher, S. 2008. *Phase I Regional Geology, Southern Ontario: OPG's Deep Geologic Repository for Low & Intermediate Level Waste*. Supporting Technical Report OPG 00216-REP-01300-00007-R00, Ontario Power Generation, Toronto, Canada.
- Golder Associates Limited. 2003. *LLW Geotechnical feasibility study, Western Waste Management Facility, Bruce site, Tiverton, Ontario*. Technical Report 021-1570, Golder Associates Limited, Toronto, Canada.
- Hobbs, M.Y., Frappe, S.K., Shouakar-Stash, O. & Kennell, L.R. 2008. *Phase I Regional Hydrogeochemistry, Southern Ontario: OPG's Deep Geologic Repository for Low & Intermediate Level Waste*. Supporting Technical Report OPG 00216-REP-01300-00006-R00, Ontario Power Generation, Toronto, Canada.
- McCauley, C.A., White, D.M., Lilly, M.R. & Nyman, D.M. 2002. A comparison of hydraulic conductivities, permeabilities and infiltration rates in frozen and unfrozen soils. *Cold Regions Science and Technology* 34(2): 117–125.
- Neuzil, C.E. 2003. Hydromechanical coupling in geologic processes. *Hydrogeology Journal* 11(1): 41–83.
- Peltier, W.R. 2008. *Phase I Long Term Climate Change Study: OPG's Deep Geologic Repository for Low & Intermediate Level Waste*. Supporting Technical Report OPG 00216-REP-01300-00004-R00, Ontario Power Generation, Toronto, Canada.
- Sykes, J.F., Sykes, E.A., Normani, S.D., Yin, Y. & Park, Y.J. 2008. *Phase I Hydrogeologic Modelling: OPG's Deep Geologic Repository for Low & Intermediate Level Waste*. Supporting Technical Report OPG 00216-REP-01300-00009-R00, Ontario Power Generation, Toronto, Canada.
- Therrien, R., Sudicky, E.A. & McLaren, R.G. 2004. *FRAC3DVS: An Efficient Simulator for Three-dimensional, Saturated-Unsaturated Groundwater Flow and Density-dependent, Chain-Decay Solute Transport in Porous, Discretely-Fractured Porous or Dual-porosity Formations. User's Guide*. Groundwater Simulations Group, University of Waterloo, Waterloo, Ontario, Canada.